Materials Advances

ROYAL SOCIETY OF CHEMISTRY

PAPER

View Article Online
View Journal | View Issue

Check for updates

Cite this: *Mater. Adv.*, 2022, 3, 5393

A novel ion-responsive photonic hydrogel sensor for portable visual detection and timely removal of lead ions in water†

Zhuo Peng, [a] Hai-Rong Yu, *[ab] Jing-Ya Wen, [a] Yan-Lin Wang, [a] Ting Liang [ab] and Chang-Jing Cheng *[ab]

Lead-ion (Pb^{2+}) contamination is a serious environmental problem worldwide. Although various methods have been developed for the detection or removal of Pb^{2+} in water environments, the availability of techniques with the capability of both highly selective, visual monitoring and timely separation remains a challenge. Herein we report a novel ion-responsive photonic hydrogel sensor based on the poly(*N*-isopropylacrylamide-*co*-benzo-18-crown-6-acrylamide) (PNBC) hydrogel with embedded orderly Fe_3O_4 colloidal nanocrystal cluster (CNC) chains, for highly selective and portable visual detection of Pb^{2+} by the naked eye, and the effective elimination of Pb^{2+} in aqueous solutions. The pendent 18-crown-6 units in the hydrogel backbone act as ion-responsive receptors to form B18C6Am/Pb^{2+} host–guest inclusion complexes with Pb^{2+} in water, while the poly(*N*-isopropylacrylamide) (PNIPAM) moieties serve as thermosensitive actuators to regulate the inclusion constants of the B18C6Am/Pb^{2+} complexes, which significantly affect the volume of the hydrogel. The fixed Fe_3O_4 CNC chains function as optical signal transmitters that can diffract visible light, thus endowing the hydrogel with bright structural colors. The osmotic pressure and swelling of the PNBC hydrogel can induce an increase in lattice spacing of the Fe_3O_4 CNCs when Pb^{2+} is selectively captured by the 18-crown-6 units, thus triggering a redshift in the diffraction wavelength and showing structural color changes of the PNBC hydrogel according to the Bragg diffraction law. Correspondingly, highly selective Pb^{2+} detection can be realized by the Pb^{2+}-induced diffraction-wavelength shifts or direct observation of the color changes of the hydrogel by the naked eye. Furthermore, such a functional hydrogel sensor can simultaneously adsorb Pb^{2+} from aqueous solution and the Freundlich isotherm model fits well with the adsorption process. Most importantly, the facile and complete regeneration of the photonic hydrogel sensor can be easily achieved by simply changing the operating temperature to release the bound Pb^{2+} from the 18-crown-6 units based on the excellent thermosensitivity of the PNIPAM moieties. Such a novel photonic hydrogel sensor with high selectivity, portable visual detection and an excellent removal performance toward Pb^{2+} in water, as well as excellent regenerability, holds great promise for the monitoring and remediation of environmental pollutants.

Received 28th February 2022,
Accepted 5th May 2022

DOI: 10.1039/d2ma00232a

rsc.li/materials-advances

Introduction

Lead ions (Pb^{2+}) are one of the most stable and toxic heavy metal ions, which pose a constant threat to human beings through their enrichment in the environment (*i.e.*, in soil, air, and water). Because of its excellent physical properties of low melting point and high ductility, Pb has been widely utilized in many fields including mining, smelting, refining, and battery manufacture.[1] It is easy for Pb^{2+} to enter the human body through food, air, water or skin contact and these ions accumulate in vital organs and tissues *via* the gastrointestinal and respiratory systems.[2] Even at a low concentration, Pb^{2+} can cause serious damage to human health such as the nervous system, immune system, and digestive system.[1,2] Therefore, the effective detection and timely removal of Pb^{2+} in aqueous environments is extremely significant and urgent. Currently, some conventional methods including atomic adsorption spectrometry,[3] electrochemical methods,[4] and inductively

[a] *College of Chemistry and Environment, Southwest Minzu University, Chengdu, Sichuan 610041, China. E-mail: yuhr@swun.edu.cn, chengcj@swun.edu.cn*
[b] *Key Laboratory of Pollution Control Chemistry and Environmental Functional Materials for Qinghai-Tibet Plateau of the National Ethnic Affairs Commission, College of Chemistry and Environment, Southwest Minzu University, Chengdu, Sichuan 610041, China*

† Electronic supplementary information (ESI) available. See DOI: https://doi.org/10.1039/d2ma00232a

coupled plasma-mass spectrometry (ICP-MS)[5] have been developed for Pb^{2+} detection. These have shown high sensitivity and accuracy, although they display disadvantages including the requirement of expensive instruments or equipment, complicated and time-consuming sample pretreatment, and professional personnel at appointed laboratories, which greatly restrict their wide application.[6–8] Moreover, the timely elimination of Pb^{2+} from contaminated water is also necessary in practical applications. Therefore, exploring a simple, low-cost method or material for the detection and removal of Pb^{2+} in water is highly urgent and desirable.

So far, various functional materials or devices, such as fluorescent probes, DNAzymes, nanogels, diffraction gratings, aerogels, and clay materials, have been developed for real-time detection or elimination of Pb^{2+} in water.[6–13] For example, Sharma *et al.* designed a sensitive fluorescent probe based on functionalized molybdenum disulfide (MoS_2) quantum dots for Pb^{2+} monitoring with a detection limit of 50 μM.[6] Fu *et al.* developed a label-free DNAzyme biosensor for amplified ''turn-on'' fluorescence sensing of Pb^{2+} with a detection limit of 3 nM.[7] Chen *et al.* designed a simple and portable device using a poly(NIPAM-*co*-B18C6Am) hydrogel and polyethylene (PE) membrane as the sensor and actuator, where the colored liquid column in the channel acts as an indicator for the visual detection of Pb^{2+}.[8] Peng *et al.* developed an ultrasensitive diffraction grating based on poly(NIPAM-*co*-B18C6Am) hydrogels for the highly selective and rapid monitoring of trace amounts of Pb^{2+} in water at concentrations as low as 10^{-9} M.[9] Liu *et al.* constructed an osmosis-driven liquid column loaded with poly(NIPAM-*co*-B18C6Am) smart nanogels for the visual detection of trace Pb^{2+} in aqueous solution.[10] Besides, Ju *et al.* designed poly(NIPAM-*co*-BCAm) hydrogels to remove Pb^{2+} from aqueous solutions, which showed good ion recognition and adsorption properties.[11] Bai *et al.* reported the adsorption of copper ions (Cu^{2+}) and Pb^{2+} from wastewater using an aerogel formed from functionalized poplar catkins.[12] Chen *et al.* studied the removal of Pb^{2+} from aqueous solutions using both modified and unmodified kaolinite clays.[13] Although these materials or devices show reasonable detection or adsorption performances toward Pb^{2+}, there have been few reports on the simultaneous portable, naked-eye visual detection and timely removal of Pb^{2+} in water. Hence, developing one novel functional material aimed at effective visual monitoring and timely elimination of Pb^{2+} in water is highly desirable.

Photonic crystals (PCs) are a class of novel optical materials with periodic micro-/nano-structures that possess a photonic bandgap to control and manipulate the flow of light in the visible region and thus exhibit bright structural colors.[14–17] Fixing colloidal PCs, such as monodisperse polystyrene (PS),[18–21] silica (SiO_2),[22,23] and superparamagnetic colloidal nanoparticles,[24–26] in responsive polymers brings about responsive photonic hydrogels (RPHs), which have the capability of

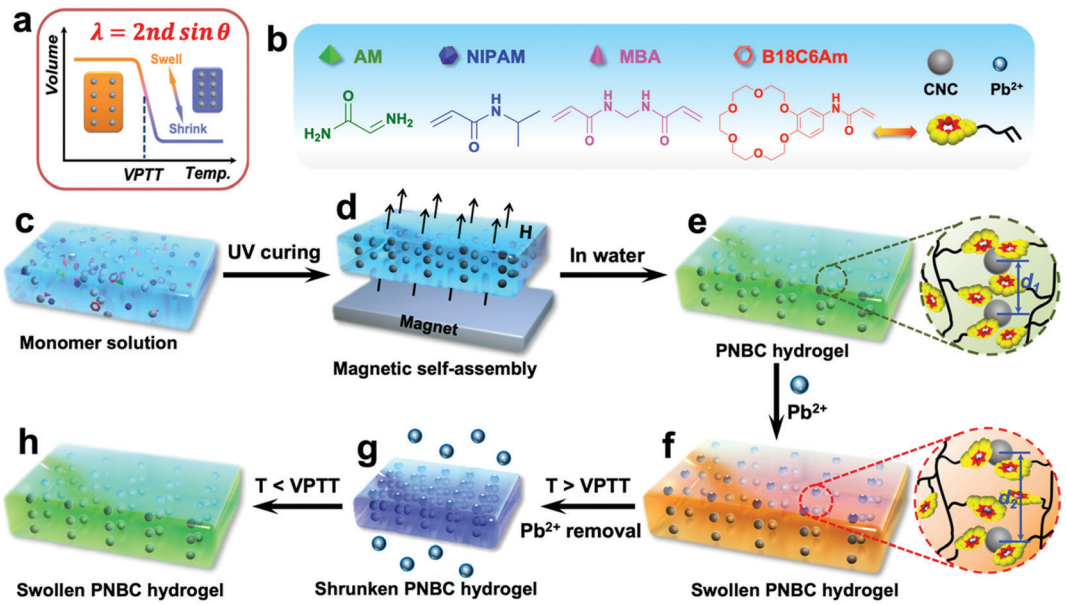

Fig. 1 Schematic illustration of the fabrication, detection, adsorption and regeneration process of the PNBC hydrogel sensor toward Pb^{2+} in aqueous solution. (a) The volume shrinkage of the PNBC hydrogel sensor triggers the structural color change as the operating temperature increases across its volume phase transition temperature (VPTT). (b and c) The precursor solution contains superparamagnetic Fe_3O_4 CNCs, B18C6Am, NIPAM, and AM as monomers, and MBA as the crosslinker. (d) Fe_3O_4 CNCs in the precursor solution self-assemble into a 1D stable chainlike structure under an EMF and then the PNBC hydrogel sensor is obtained *via* rapid UV curing. (e) The prepared PNBC hydrogel sensor is washed by immersing it in water and swells fully at room temperature. (f) The hydrogel expands its volume isothermally in response to any Pb^{2+} in the water, and thus exhibits different structural colors in Pb^{2+} solutions at various concentrations due to variation of the lattice spacing. (g and h) Meanwhile, Pb^{2+} ions are specifically recognized and captured by 18-crown-6 units to form B18C6Am/Pb^{2+} complexes, thus removing them from the environment. By simply raising the operating temperature above the VPTT, Pb^{2+} ions undergo decomplexation from the crown ether cavities, after which complete regeneration of the PNBC hydrogel can be achieved in a facile manner.

adjusting the lattice spacing among the embedded PC particles in response to the volume change of hydrogels (swelling or shrinkage) caused by various external stimuli (temperature, humidity, pressure, pH, ions, molecules, and bacteria),[27–34] thus generating various brilliant colors. Such RPHs with embedded PCs do not suffer from photobleaching, and their striking advantage of having colourfast, highly stable, bright colors enable them to be ideal colorimetric detection devices compared with other sensing platforms. For example, Asher and co-workers initiatively proposed the immobilization of crystal colloidal arrays (PS CCAs) in responsive hydrogels to obtain a series of smart sensing materials.[18,35–37] Zhang *et al.* designed photonic polyelectrolyte hydrogels for specific metal-ion sensing by combining three-dimensional (3D)-ordered SiO_2 interconnected macroporous structures and ligand preorganization.[22] The unique properties of RPHs have enabled them to become novel visual sensing materials with the advantage of direct readout *via* the naked eye for the sensitive colorimetric detection of a variety of target analyses that include heavy metal ions (Pb^{2+}, Be^{2+}, Ni^{2+}, Hg^{2+}, and Cd^{2+}).[18,19,36,38,39] The concentrations of the target ions can trigger diffraction-wavelength shifts, thus bringing about structural color changes of the functional materials. This has been utilized in the portable colorimetric detection of various object analytes. However, some challenges remain, including the complicated fabrication process, high expense and unsatisfactory detection performance. Besides, although 18-crown-6-based PC sensing materials have been reported for investigation of the responsive characteristics of Pb^{2+},[37,40,41] and poly(NIPAM-*co*-B18C6Am)-based hydrogels or functional membranes[42–44] have been reported for the detection or removal of Pb^{2+} from aqueous environments, it is still unknown whether such poly(NIPAM-*co*-B18C6Am)-based hydrogels integrated with PCs as a unitary material can both detect trace Pb^{2+} levels and eliminate them from water in a timely fashion. If a unitary material can be developed to specifically and selectively detect and simultaneously remove Pb^{2+} in water, and the regeneration of the material can be achieved by simply changing the operating temperature and washing with water after use, this will be more beneficial to its practical applications.

Herein we report a novel ion-responsive photonic hydrogel sensor for the highly selective, point-of-care colorimetric detection and removal of Pb^{2+} in aqueous solution. This sensor is composed of the poly(*N*-isopropylacrylamide-*co*-benzo-18-crown-6 acrylamide) (PNBC) hydrogel with embedded Fe_3O_4 CNC chains. The bound 18-crown-6 units in the hydrogel backbone act as Pb^{2+}-responsive receptors that are capable of forming B18C6Am/Pb^{2+} host–guest inclusion complexes with Pb^{2+} in water, while the poly(*N*-isopropylacrylamide) (PNIPAM) moieties serve as thermosensitive actuators to regulate the inclusion constants of the B18C6Am/Pb^{2+} complexes, thus significantly affecting the volume of the hydrogel (Fig. 1a).[11,35,40,43,44] Moreover, the fixed Fe_3O_4 CNC chains function as optical signal transmitters and can diffract visible light, thereby endowing the prepared functional hydrogel with bright structural colors.[14,24] Fig. 1 shows the schematic illustration of the fabrication, detection, and adsorption and regeneration process of the photonic hydrogel sensor toward Pb^{2+} in aqueous solution. The superparamagnetic Fe_3O_4 CNCs obtained *via* a versatile solvothermal reaction are first dispersed in ethylene glycol solution that contains functional monomers of benzo-18-crown-6 acrylamide (B18C6Am), *N*-isopropylacrylamide (NIPAM), and acrylamide (AM) as well as the crosslinker of *N*,*N*′-methylenediacrylamide (MBA) (Fig. 1b and c), which can self-assemble into one-dimensional (1D) periodic nanochains under an EMF, which are subsequently embedded in the hydrogel *via* rapid UV curing (4 min) (Fig. 1d and e). If the surrounding operating temperature is below the volume phase transition temperature (VPTT) of the hydrogel, Pb^{2+} ions in the water are specifically recognized and captured by the 18-crown-6 units to form stable, positively charged B18C6Am/Pb^{2+} complexes and are simultaneously removed (Fig. 1f). The PNBC hydrogel undergoes isothermal hydrophobic-to-hydrophilic transitions and appears in the swollen state.[45] The volume changes of the hydrogel can trigger an increase in the lattice spacing (from d_1 to d_2) of the embedded Fe_3O_4 CNCs (Fig. 1e and f), and thus redshift of the diffraction wavelengths occurs.[17,26,40] The PNBC hydrogel can specifically capture Pb^{2+} *via* the 18-crown-6 units and automatically converts the signal into a visually perceptible color change (Fig. 1e and f). After complexation of Pb^{2+} with the crown ether molecules reaches saturation, the bound Pb^{2+} ions undergo decomplexation from the crown ether cavities upon the thermo-induced reduction in the inclusion constants by simply increasing the operating temperature to above the VPTT.[44,46] Meanwhile, the PNBC hydrogel shrinks and dehydrates (Fig. 1g). Besides, when the environmental temperature is reduced to room temperature, the hydrogel color reversibly recovers its original color (bright green) when immersed in water (Fig. 1h). This facile regeneration process for photonic hydrogel materials simply by changing the environmental temperature without compromising its detection or adsorption performance endows our strategy with notable advantages, including simplicity of operation, inexpensiveness and environmental friendliness. Such a hydrogel sensor with high selectivity, portability and colorimetric detection by the naked eye, as well as the removal of Pb^{2+} from water and excellent regenerability hold great promise for the monitoring and remediation of environmental pollutants.

Experimental

Materials

Poly(4-styrenesulfonic acid-*co*-maleic acid) sodium salt (PSSMA (SS : MA = 3 : 1), M_w = 20 000) and 2-hydroxy-2-methylpropiophenone (HMPP) were bought from Aladdin Chemicals (Shanghai, China). *N*-Isopropylacrylamide (NIPAM) obtained from TCI (Shanghai, China) was purified through recrystallization using a mixture of hexane and acetone (v/v, 50/50). Benzo-18-crown-6 acrylamide (B18C6Am) was synthesized from 4′-nitrobenzo-18-crown-6 (NB18C6; TCI) according to ref. 47 and 48. *N*,*N*′-Methylenediacrylamide (MBA), sodium acetate trihydrate (NaAc·$3H_2O$), acrylamide (AM), ferric chloride hexahydrate ($FeCl_3$·$6H_2O$) and various nitrates including $Pb(NO_3)_2$, $Mg(NO_3)_2$, $Co(NO_3)_2$, $Ca(NO_3)_2$, $Cd(NO_3)_2$, $CsNO_3$, $Zn(NO_3)_2$, $Cu(NO_3)_2$,

$Ni(NO_3)_2$, $NaNO_3$, and KNO_3 were all purchased from Kelong Chemicals (Chengdu, China). Nitrates were dissolved in deionized water as metal-ion solution samples. All other chemicals were of analytical grade and used as received. Deionized water (18.2 MΩ, 25 °C) from a Milli-Q plus water purification system (Millipore) was used throughout this work.

Synthesis of superparamagnetic Fe_3O_4 CNCs

Superparamagnetic Fe_3O_4 CNCs with a hydrodynamic diameter of ~158 nm were synthesized *via* a versatile solvothermal reaction according to our recent work.[49] Typically, 2.5 g of PSSMA (3 : 1) serving as the stabilizer and 0.596 g of $FeCl_3{\cdot}6H_2O$ were added successively to 40 mL of ethylene glycol (EG) to form a homogeneous solution under vigorous mechanical stirring for 20 min. Then, 3.0 g of $NaAc{\cdot}3H_2O$ was rapidly added under continuous stirring for another 20 min. After forming a transparent brownish-red solution, the mixture was transferred into a 100 mL Teflon-lined stainless-steel autoclave and reacted at 200 °C for 10 h. The product was collected using a magnet and washed with excessive water and then dispersed in 20 mL of water for further use.

Synthesis of PNBC photonic hydrogel sensor

The thermo- and Pb^{2+}-responsive poly(*N*-isopropylacrylamide-*co*-benzo-18-crown-6-acrylamide) (PNBC) photonic hydrogel sensor was fabricated *via* rapid UV curing of the precursor solution containing functional monomers, crosslinker and photoinitiator in the presence of the self-assembled Fe_3O_4 CNC nanochains under an EMF. In detail, the monomers which included B18C6Am (50 mg), NIPAM (90 mg) and AM (60 mg), the MBA crosslinker (0.8 mg), the HMPP photoinitiator (10 μL), and 0.5 mL of Fe_3O_4 CNCs were mixed with 0.17 mL of EG assisted by intense sonication to obtain a homogeneous precursor solution. Then, the precursor solution was gently injected into self-made quartz glass grooves with different dimensions (250 and 500 μm in thickness, 2.0 cm × 2.0 cm in length and width) and covered with a quartz glass slide. The glass reaction grooves were placed vertically 2.5 cm above a NdFeB magnet (10 cm × 10 cm × 1 cm) with a magnetic field strength of 220 Gs measured using a digital Gauss meter (HT20/HT20A). After exposing the precursor solution to UV light (365 nm, 400 W) for 4 min, the PNBC photonic hydrogel sensor with a purple color was obtained, this was flushed to remove the unreacted chemicals and then soaked in water for subsequent experiments.

Characterization

The morphology and size of the as-synthesized Fe_3O_4 CNCs were characterized using a transmission electron microscope (TEM; JEM-2010, JEOL, Japan) at an accelerating voltage of 120 kV. The sample at an appropriate concentration was added dropwise onto a carbon-coated copper grid followed by air-drying. The hydrodynamic diameter of the Fe_3O_4 CNCs in water was measured using a dynamic light scattering (DLS) instrument (Zetasizer Nano-ZS, Malvern Instruments, UK) at 25 °C. The morphologies and elemental analysis of the freeze-dried PNBC photonic hydrogel were carried out using a scanning electron microscope (SEM; Thermo Scientific, Apreo 2C, Czech) equipped with an energy dispersive spectroscopy (EDS) unit after sputter-coating the samples with gold. Before characterization, the hydrogel was rapidly immersed in liquid nitrogen to freeze it, and it was freeze-dried under vacuum for 48 h. The chemical compositions of the PNBC photonic hydrogel and B18C6Am were characterized using a Fourier transform infrared (FT-IR) spectrometer (IR 200, Thermo Nicolet, USA). The photographs and reflection spectra of the PNBC photonic hydrogel in various metal ion solutions were recorded and measured, respectively, using a cellphone (HUAWEI, Pro30, China) and a fiber optic spectrometer (FLAME-S-VIS-NIR-ES, Ocean Optics) with a spectral range of 400–900 nm. The hydrogel was equilibrated in solution for 3 h before recording, during which the angle between the optical fiber and the hydrogel was kept at 90°. A thermal analyzer (TG-DSC, Mettler Toledo, TGA/DSC^{3+}, Switzerland) was used to analyze the VPTT of the prepared hydrogel from 25 to 150 °C at a heating rate of 10 °C min^{-1} under a N_2 atmosphere.

Point-of-care visual detection of Pb^{2+} using the PNBC photonic hydrogel sensor

Typically, the PNBC photonic hydrogel sensor with a size of 3.5 cm × 3.5 cm was immersed in 50 mL Pb^{2+} aqueous solution (pH = 5.5) at various concentrations for 3 h at 25 °C. After reaching equilibrium, the structural colors of the hydrogel were observed with the naked eye and recorded using the cellphone. The diffraction wavelengths of the hydrogel were measured using the fiber optic spectrometer. The differences in the diffraction wavelength shifts in Pb^{2+} aqueous solution and water were defined as $\Delta\lambda$. To study the effect of the response time on the Pb^{2+}-detection behavior of the PNBC photonic hydrogel, the 500-μm-thick hydrogel was soaked in 1 and 5 mM Pb^{2+} solutions for point-of-care detection, respectively. To evaluate the effect of the hydrogel thickness on the sensing performance, the 250-μm-thick hydrogel was also immersed in 5 mM Pb^{2+} solutions for in-time detection. The $\Delta\lambda$ values at predetermined time intervals were also measured using the fiber optic spectrometer.

Since the PNIPAM moieties within the PNBC hydrogel have thermo-responsiveness, which may affect the Pb^{2+}-detection performance, the thermosensitivity of the PNBC photonic hydrogel as well as the effect of temperature on the Pb^{2+}-detection behavior were investigated. The swollen hydrogel was immersed in 5 mM Pb^{2+} solution at various temperatures from 25 to 80 °C, and the container was placed in a thermostatic water bath (CH1015, China) for 3 h at each predetermined temperature. The thermo-induced diffraction wavelength shifts of the hydrogel were recorded after the hydrogel reached equilibrium and the corresponding $\Delta\lambda$ was calculated. The effect of the solution pH on the Pb^{2+}-detection behavior was also studied. The hydrogel was soaked in 5 mM Pb^{2+} solutions at various pH values before the $\Delta\lambda$ of the hydrogel was recorded. The solution pH values were adjusted from 2 to 7 using 0.1 M hydrochloric acid (HCl) or ammonium hydroxide ($NH_3{\cdot}H_2O$).

To study the Pb^{2+} detection selectivity of the PNBC photonic hydrogel, the hydrogel was soaked in water containing various metal ions. The Pb^{2+} as well as the interfering ions, which included K^+, Na^+, Cs^+, Ca^{2+}, Mg^{2+}, Ni^{2+}, Cu^{2+}, Zn^{2+}, Cd^{2+}, or Co^{2+} at a concentration of 5 mM for each ion, were separately added to the solutions to measure the $\Delta\lambda$. Moreover, the Pb^{2+} solutions containing complex interfering ions of K^+, Na^+, Mg^{2+}, and Ca^{2+} were used for further investigation of the selective monitoring of Pb^{2+} at a concentration of 1 mM, while varying the concentration of each interfering ion from 1 to 100 mM. In addition, the Pb^{2+} detection performance and selectivity for actual environmental water samples were further verified by adding different concentrations of Pb^{2+} to tap-water samples. To study the reusability of the PNBC photonic hydrogel sensor, the used hydrogel after Pb^{2+} detection or adsorption was alternately washed with cold/hot (25 and 75 °C) water several times before being reused for the next cycle of Pb^{2+} monitoring (C_0 = 5 mM). The diffraction wavelengths were obtained in the same way as described above.

Adsorption of Pb^{2+} by the PNBC photonic hydrogel sensor

The adsorption of Pb^{2+} by the PNBC photonic hydrogel sensor was carried out by adding 0.14 g of dried PNBC hydrogel to 10 mL of Pb^{2+} aqueous solutions at various concentrations. The sealed container was placed in a thermostatic shaker with a vibrating speed of 100 rpm and at 25 °C for 12 h to reach adsorption equilibrium. The hydrogel was separated using a filter and the concentration of Pb^{2+} in the filtrate before and after adsorption was measured using inductively coupled plasma-mass spectrometry (ICP-MS; Thermo Fisher Scientific). All the adsorption experiments were performed at least thrice to ensure the precision of the data analysis.

Results and discussion

Characterization of the PNBC photonic hydrogel

As shown in Fig. 2a, the typical SEM image of the cross-section of the hydrogel shows the formation of an internal network structure and macropores within the freeze-dried hydrogel. The free water inside the swelling hydrogel turns into ice crystals and then sublimates to form numerous macropores in the hydrogel during the freeze-drying process.[50] The amplified SEM images of the hydrogel clearly show the 1D chainlike microstructures of the superparamagnetic Fe_3O_4 CNCs inside the hydrogel (Fig. 2b and c), which arise *via* self-assembly of Fe_3O_4 CNCs under an EMF, and which serve as optical signal transmitters that can diffract visible light, thus endowing the functional hydrogel with brilliant structural colors.[25,26,28,35,49] Since the precursor solution contains hydrophilic functional monomers like NIPAM, AM, and B18C6Am, the copolymer chains of the PNBC photonic hydrogel can easily expand and become hydrophilic. Therefore, the hydrogel exhibits significant volume expansion in water, which leads to some folds being produced inside the network structure when the free water within the swelling hydrogel turns into ice crystals, forming numerous macropores during the freeze-drying process, making the Fe_3O_4 CNCs chains particularly non-uniform in the hydrogel. Furthermore, the digital image of the hydrogel

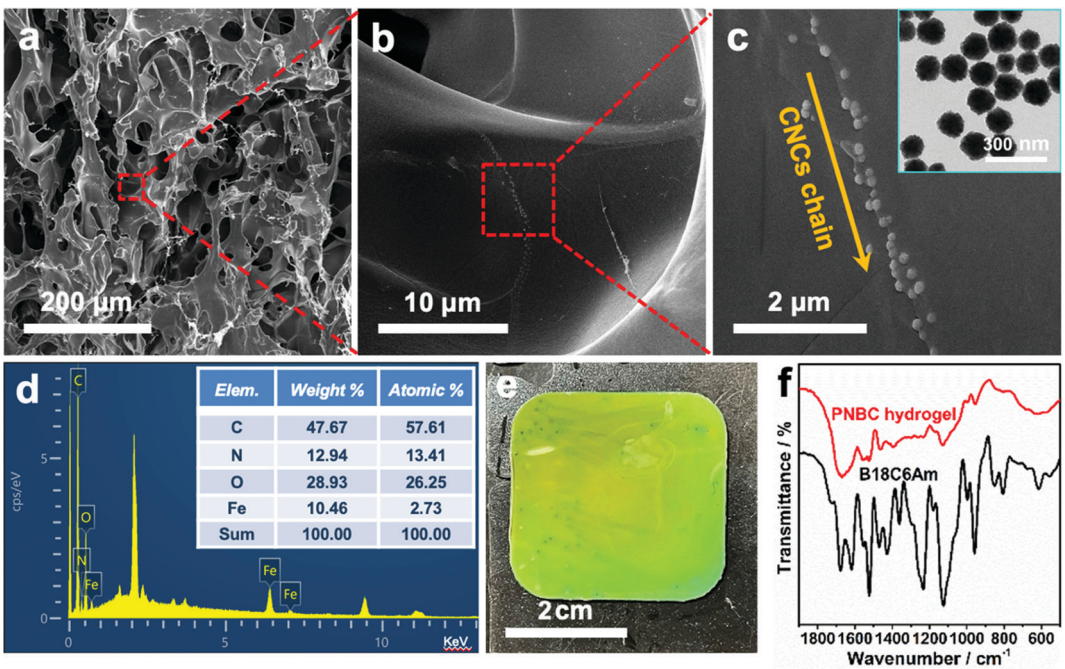

Fig. 2 Characterization of the PNBC photonic hydrogel sensor. (a) Cross-sectional SEM image of the PNBC hydrogel and (b and c) the 1D chainlike structure of the superparamagnetic Fe_3O_4 CNCs within the PNBC hydrogel. The inset in (c) shows the TEM image of the as-synthesized Fe_3O_4 CNCs. (d) EDS spectrum and elemental analysis of the PNBC hydrogel for the red dashed box in (a). (e) Photograph of the PNBC hydrogel. (f) FT-IR spectra of the PNBC hydrogel and B18C6Am monomer.

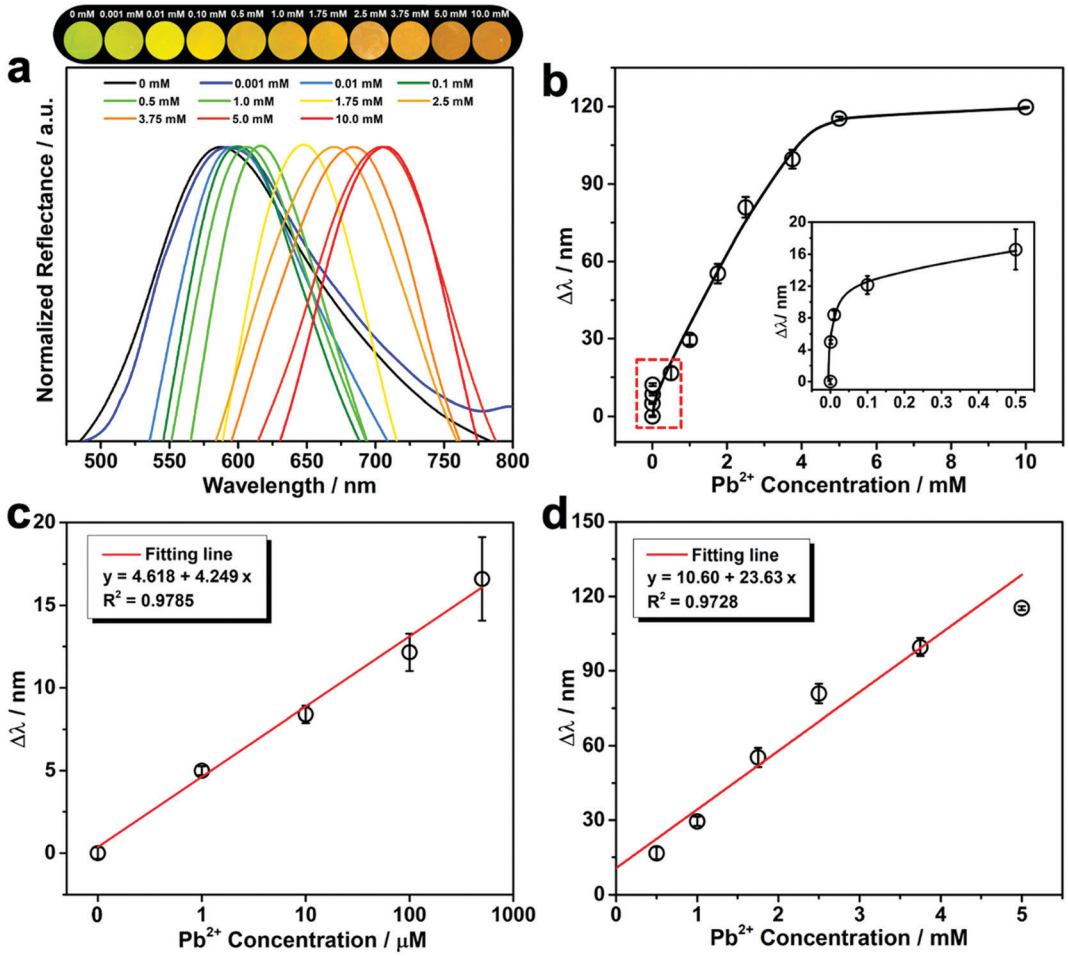

Fig. 3 (a) Photographs (top) and reflection spectra of the PNBC photonic hydrogel sensor (bottom) in response to Pb^{2+} solutions where the concentration is varied from 0 to 10 mM. (b) Calibration curve of the diffraction wavelength shift ($\Delta\lambda$) *versus* the Pb^{2+} concentration. The linear relationships between $\Delta\lambda$ and the corresponding Pb^{2+} concentration ranging from 1 to 500 μM (c) and from 0.5 to 5 mM (d). Fitting lines are shown in red. The operating temperature is 25 °C, and the solution pH value is 5.5.

shows that the color is slightly inhomogeneous (Fig. 2e), indicating that slight aggregations of the Fe_3O_4 CNC chains took place (Fig. 2c).

This may be due to the high concentration of Fe_3O_4 CNCs in the monomer solution. Under an EMF, the magnetic field gradient causes the individual magnetic Fe_3O_4 CNC chains to aggregate, thus bringing these single chains very close to each other in solution and eventually disordering some individual chains upon UV photopolymerization. Tang *et al.* also observed a similar phenomenon when preparing a magnetochromic photonic hydrogel.[51] The resulting Fe_3O_4 CNCs are nearly monodisperse and spherical with an average diameter of ~130 nm (the inset in Fig. 1c). The 10.46% weight of the iron element appears in the hydrogel (the inset table in Fig. 2d) further confirming that the Fe_3O_4 CNCs have been successfully embedded within the hydrogel after rapid UV curing. Besides, the successful fabrication of the PNBC photonic hydrogel sensor was also verified *via* FT-IR results (Fig. 2f). Specifically, the C=C skeletal stretching vibration in the phenyl ring at 1521 cm^{-1}, the asymmetric stretching vibration of C–O in Ar–O–R at 1234 cm^{-1}, and the asymmetric stretching vibration of C–O in the R–O–R groups at 1125 cm^{-1} are observed from the spectrum of B18C6Am. These peaks also appear in the FT-IR spectrum of the PNBC photonic hydrogel. The double peaks at 1361 and 1393 cm^{-1}, and the C=O stretching vibration at 1645 cm^{-1} for the PNIPAM moieties within the hydrogel are also witnessed. These results verify again the successful fabrication of the PNBC photonic hydrogel sensor.

Visual detection of Pb^{2+} using the PNBC photonic hydrogel sensor

As shown in Fig. 3a, after immersing the PNBC photonic hydrogel in Pb^{2+} solutions at various concentrations, the hydrogel shows evident diffraction wavelength redshifts and exhibits bright structural colors as observed by the naked eye. This is because the fixed Fe_3O_4 CNC chains embedded the hydrogel diffract the incident light.[25,26,28,35,54] The pendent 18-crown-6 units in the hydrogel backbones specifically recognize and capture Pb^{2+} ions to form stable 1 : 1 B18C6Am/Pb^{2+} host–guest inclusion complexes,[11,44] thus generating an osmotic pressure

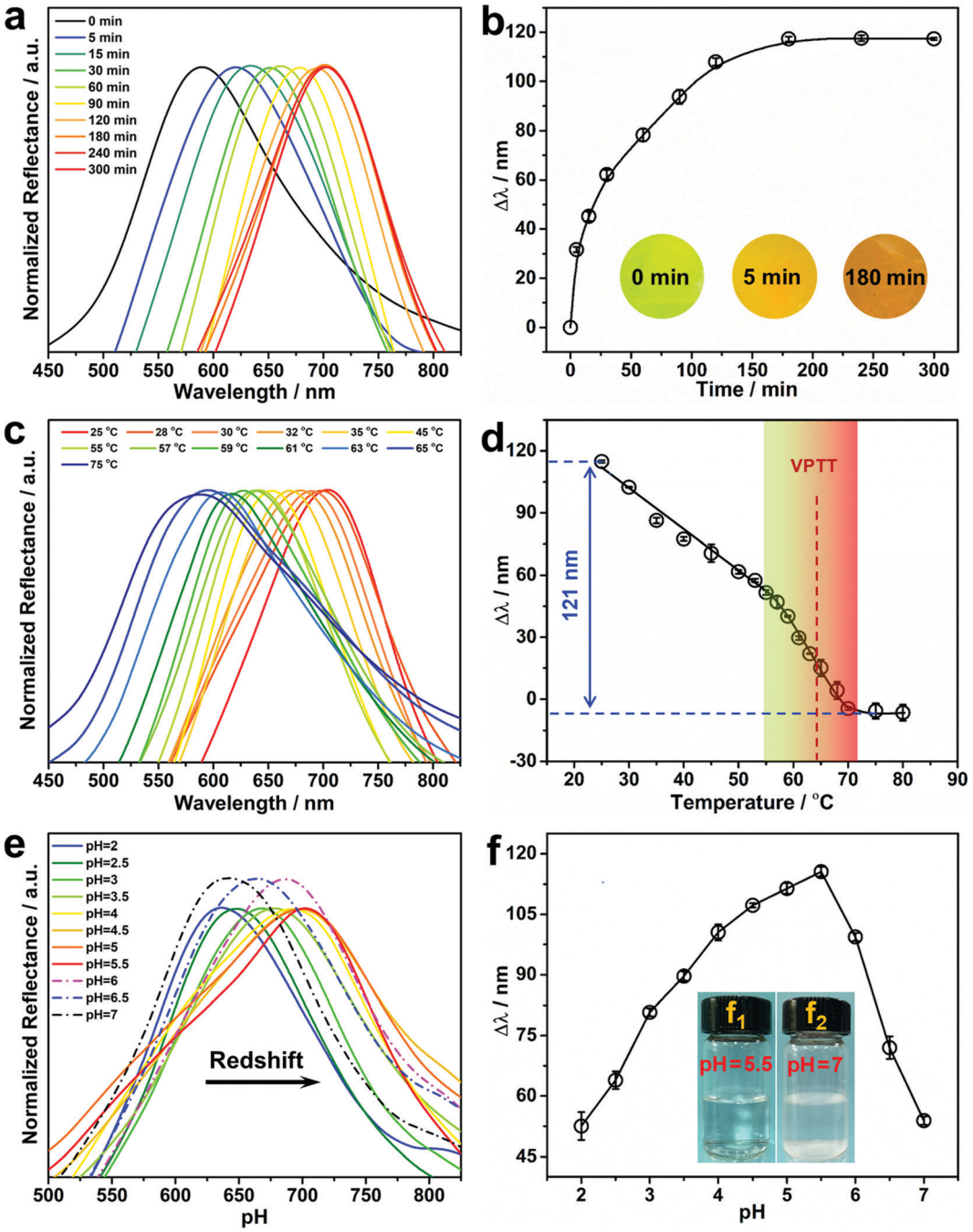

Fig. 4 (a) Reflection spectra and (b) the $\Delta\lambda$ of the PNBC hydrogel in 5 mM Pb^{2+} solution for different times. (c and d) Effect of the operating temperature on the reflection spectra and $\Delta\lambda$ of the PNBC hydrogel in 5 mM Pb^{2+} solution. (e and f) Effect of the solution pH on the reflection spectra and $\Delta\lambda$ of the PNBC hydrogel in 5 mM Pb^{2+} solution at an operating temperature of 25 °C. The thickness of the PNBC hydrogel is 500 μm. The insets (f_1 and f_2) show the transparent (pH = 5.5) and opaque (pH = 7) aqueous solutions of Pb^{2+} (5 mM), respectively.

due to the Donnan potential and causing swelling of the hydrogel.[40,52] Such a volume change of the hydrogel triggers an increase in the lattice spacing of the fixed Fe_3O_4 CNCs, thus causing the redshift of the diffraction wavelength.[25,26,53,54] The calibration curve of the diffraction wavelength shift ($\Delta\lambda$) *versus* the Pb^{2+} concentration is displayed in Fig. 3b. The diffraction peak gradually redshifts to larger values from 587 to 705 nm ($\Delta\lambda$ = 118 nm) with increasing the Pb^{2+} concentrations from 0.001 to 5 mM. With a further enhance in the Pb^{2+} concentration to 10 mM, there is no obvious redshift in the diffraction wavelengths or any structural color change of the hydrogel observed, showing that there is a quantitative relationship between $\Delta\lambda$ and the Pb^{2+} concentration over a certain concentration range.[37,55] It is worth noting that $\Delta\lambda$ and the corresponding concentration of Pb^{2+} show a linear relationship over certain concentration ranges (Fig. 3c and d). The linear detection

scopes of the PNBC hydrogel are in the ranges of ~1–500 μM for low-concentration solutions (Fig. 3c) and 0.5–5 mM for high-concentration solutions (Fig. 3d). The corresponding slopes of the fitting lines are 4.249 and 23.63, respectively, and the correlation coefficients (R^2) are larger than 0.972, showing a good linear relationship.[33] Through the linear diagrams of $\Delta\lambda$ as a function of the Pb^{2+} concentration, the Pb^{2+} concentration can be conveniently and quickly determined. This is extremely beneficial for obtaining the concentration of toxic heavy metal ions in water media. Furthermore, the $\Delta\lambda$ value can be easily observed, even for a trace of Pb^{2+} in water (1 μM) (the inset in Fig. 3b), lower than the discharge standard of lead in wastewater (about 2.4 μM).[2] That is to say, Pb^{2+} detection can be easily achieved using our developed photonic hydrogel sensor over a relatively wide concentration range (1 μM to 5 mM).

Effect of contact time on the Pb^{2+} detection performance

The concentration of Pb^{2+} in aqueous solution significantly affects its diffusion into the hydrogel, and thus has a remarkable impact on the response rate of the PNBC hydrogel (swelling or shrinkage), and thus its structural color. Therefore, the hydrogel with a thickness of 500 μm was soaked in Pb^{2+} solutions with concentrations of 1 and 5 mM to explore the point-of-care monitoring of Pb^{2+}. As shown in Fig. 4a and b, the PNBC hydrogel responds quickly within the initial 90 min and the $\Delta\lambda$ value reaches about 91 nm at a higher Pb^{2+} concentration (5 mM), and then increases slowly up to 116 nm after 180 min. It is worth noting that the hydrogel colors change rapidly from green to light orange within the first 5 min, for which the $\Delta\lambda$ value reaches around 31 nm (Fig. 4b). By contrast, the $\Delta\lambda$ value in a 1 mM Pb^{2+} solution is only 26 nm within the first 90 min and then increases little, where the final wavelength shift is only 28 nm after 120 min (Fig. S1 in the ESI†). For the same contact time, the $\Delta\lambda$ value in the 5 mM Pb^{2+} solution is much larger than that in the 1 mM Pb^{2+} solution. This can be explained since, at a low Pb^{2+} concentration, it takes more time for Pb^{2+} to diffuse into the interior of the hydrogel due to the osmotic pressures that arise from the difference in concentrations of mobile ions inside and outside the hydrogel.[19,56] Therefore, a contact time of 180 min was chosen for the subsequent experiments. Besides, the $\Delta\lambda$ value of the control PNBC hydrogel with a thickness of 250 μm in response to the 5 mM Pb^{2+} solution is shown in Fig. S2 (ESI†). As observed, the 250-μm-thick PNBC hydrogel shows a faster response to Pb^{2+} compared with the thicker sample (500 μm) (Fig. 4b). The $\Delta\lambda$ value rapidly reaches around 13 nm within just tens of seconds, and the color of the hydrogel changes from dark green to yellow green after a few minutes. This is because the transfer and infiltration of Pb^{2+} are faster for a less thick hydrogel at a fixed time, thus showing a more rapid sensing.[38] However, as the thickness of the hydrogel is decreased, the light transmittance of the hydrogel increases, so the color of the hydrogel becomes darker and the $\Delta\lambda$ value is only about 30 nm after 180 min. By contrast, the abundant crown ether groups suspended in the loose network structure of the 500-μm-thick hydrogel can easily recognize and capture Pb^{2+} in water and interact with them to form B18C6Am/Pb^{2+} host–guest complexes, causing a larger osmotic pressure and expanding the hydrogel volume and thickness, thus showing more obvious structural color changes.[40,53,54] Although increasing the hydrogel thickness would prolong the diffusion and response time of Pb^{2+}, the 500-μm-thick PNBC hydrogel can still respond rapidly and shows significant color changes and larger wavelength shifts within 5 min. Therefore, the 500-μm-thick PNBC hydrogel was chosen in this study. It is pointed out that, although our resulting PNBC photonic hydrogel sensor is not ultrasensitive toward Pb^{2+} compared with traditional methods that depend on expensive instruments or equipment, the most distinctive advantages of our detection strategy are its simplicity of operation, its low cost, its rapidity, and its colorimetric readout that can be seen by the naked eye without requiring any professional instruments or skilled personnel operating in appointed laboratories.

Effect of temperature on the Pb^{2+} detection performance

PNIPAM-based hydrogels have attracted widespread interest due to their remarkable phase-transition behavior at temperature changes across its volume phase transition temperature (VPTT). It is conceivable that increasing the environmental temperature will result in the hydrophilic-to-hydrophobic transition of PNIPAM moieties within the PNBC hydrogel, and thus its volume variation caused by reversible hydration and dehydration,[9–11,44] thereby triggering shifts in the diffraction wavelength and structural color changes according to Bragg's diffraction law. Fig. 4c and d show the reflection spectra of the PNBC photonic hydrogel at various temperatures, and the corresponding calibration curve of $\Delta\lambda$ *versus* the solution temperature, respectively. Upon increasing the solution temperature from 25 to 75 °C, the maximum diffraction wavelength (λ_{max}) in 5 mM Pb^{2+} solution blueshifts from 703 to 582 nm ($\Delta\lambda$ = 121 nm). Raising the solution temperature enables the hydrogel to undergo a hydrophilic-to-hydrophobic transition due to the breakage of hydrogen bonds between the acylamino groups in the PNIPAM moieties and water molecules, thus shrinking the volume of the hydrogel.[9–11,44] Correspondingly, the diffraction wavelength blueshifts owing to the reduction in lattice spacing of the fixed Fe_3O_4 CNCs. Moreover, the 18 + 2 electronic structure of the 18-crown-6 units and the high polarizability of Pb^{2+} make it readily captured by the 18-crown-6 units, resulting from the strong covalent bonds with the oxygen atoms in the 18-crown-6 units to form stable B18C6Am/Pb^{2+} host–guest complexes.[57] The positively charged B18C6Am/Pb^{2+} complexes will increase the electrostatic repulsions among the copolymer chains, thereby swelling the volume of the hydrogel.[58] On the other hand, the hydrophilic B18C6Am groups can also enhance the hydrophilicity of the copolymer chains, thus making the VPTT of the hydrogel shift to a higher temperature of about 65 °C (Fig. 4d).[44,58] The PNBC hydrogel can easily recognize and capture the Pb^{2+} ions in water at room temperature (below the VPTT), resulting in an obvious shifts in the diffraction wavelength. Inclusion constants between Pb^{2+} and the 18-crown-6 units are reduced as the surrounding temperature gradually increases to a higher value than the VPTT, thus leading to release of the captured Pb^{2+}

from the 18-crown-6 cavities. Hence, the PNBC hydrogel shows a significant volume shrinking and a notable reduction in $\Delta\lambda$.

To further investigate the thermosensitivity of the PNBC hydrogel, thermogravimetric analysis of the hydrogel was performed under a N_2 atmosphere. As displayed in Fig. S3 (ESI†), the PNBC hydrogel shows a gradual weight loss of ~15.89% at a temperature of 30–150 °C due to gasification of the adsorbed water. Moreover, an evident endothermic peak at 67.33 °C is ascribed to evaporation of the adsorbed water,[59] which is consistent with the VPTT of the PNBC hydrogel (Fig. 4d). These results indicate that the prepared PNBC hydrogel retains the excellent thermosensitivity of PNIPAM. Taking advantage of the excellent thermosensitivity of the PNIPAM moieties and the ion-responsiveness of the 18-crown-6 units, the fabricated PNBC photonic hydrogel sensor can selectively and sensitively detect Pb^{2+} in water at room temperature, and achieve complete regeneration of the hydrogel sensor through a simple changing of the operating temperature.

Effect of solution pH on the Pb^{2+} detection performance

The effect of the solution pH on the Pb^{2+} detection performance of the PNBC hydrogel sensor was also studied in this work. As shown in Fig. 4e and f, when increasing the solution pH from 2 to 5.5, the diffraction wavelength of the hydrogel is gradually redshifted from 640 to 703 nm, and is then blueshifted to 642 nm ($\Delta\lambda$ = 61 nm) when the pH is further increased to 7. Hydrolysis of Pb^{2+} in aqueous solution and protonation of the ligand groups of B18C6Am for this phenomenon. Slight protonation of the B18C6Am groups at a low solution pH reduce the complexing ability to Pb^{2+}. Upon raising the solution pH from 2 to 5.5, the B18C6Am ligands gradually deprotonate, thus increasing the effective complex sites,[12,60] which makes the 18-crown-6 units bind more Pb^{2+} in solution, eventually resulting in remarkable redshifts in the structural colors of the hydrogel. However, the diffraction wavelength is blueshifted as the solution pH is increased from 5.5 to 7. This can be explained due to the formation of lead hydroxide ($Pb(OH)_2$) since the Pb^{2+} ions precipitate slightly at higher pH, above 5.5 (Fig. 4f, inset $f_1 \rightarrow f_2$).[46,60] Therefore, the solution pH was maintained at 5.5 to obtain the optimal detection performance of the PNBC hydrogel sensor in subsequent experiments.

Selectivity of Pb^{2+} detection by the PNBC photonic hydrogel sensor

The specific recognition and detection of Pb^{2+} in water by the PNBC photonic hydrogel sensor was also investigated by measuring the $\Delta\lambda$ of the hydrogel in the presence of different interfering ions at 25 °C. As observed from Fig. 5a, the $\Delta\lambda$ of the PNBC photonic hydrogel in 5 mM Pb^{2+} reaches a larger value (~117 nm), whereas for solutions without Pb^{2+} but containing one type of interfering ion (K^+, Na^+, Cs^+, Ca^{2+}, Mg^{2+}, Ni^{2+}, Cu^{2+}, Zn^{2+}, Cd^{2+} or Co^{2+}) (C_0 = 5 mM) show little effect on the $\Delta\lambda$ (less than 20 nm), even though the 18-crown-6 units are all free for ion binding. Moreover, when the solutions contain Pb^{2+}, K^+, Na^+, Mg^{2+}, and Ca^{2+} simultaneously ($C_{Pb^{2+}}$ = 1 mM, and the concentration of each interfering ion is 0, 1, 10 and 100 times as large as that of Pb^{2+}), the $\Delta\lambda$ value decreases slightly but remains almost the same as that in 1 mM Pb^{2+} solution (Fig. 5b). Therefore, we can conclude that the effect of interfering ions is negligible, even when the concentration of each interfering ion is 100 times larger than that of Pb^{2+}, indicating the high selectivity of the PNBC hydrogel toward Pb^{2+}. Compared with other metal ions like Ca^{2+}, Mg^{2+}, Ni^{2+}, Cu^{2+}, Zn^{2+}, Cd^{2+}, and Co^{2+}, the ionic radius of Pb^{2+} (1.19 Å) and the cavity size of 18-crown-6 (1.34–1.43 Å) match well, and therefore, Pb^{2+} can be tightly loaded within the cavity of 18-crown-6 *via* strong interactions.[57,61] In addition, since Pb^{2+} has a stable electronic configuration and a high polarization rate, which is favorable for the formation of stronger covalent bonds with the oxygen atoms in 18-crown-6, inclusion constants between Pb^{2+} and 18-crown-6 are much larger than those of other interfering ions ($\log K_{Pb^{2+}}$ = 3.19, $\log K_{K^+}$ = 1.74, $\log K_{Na^+}$ = 1.38,

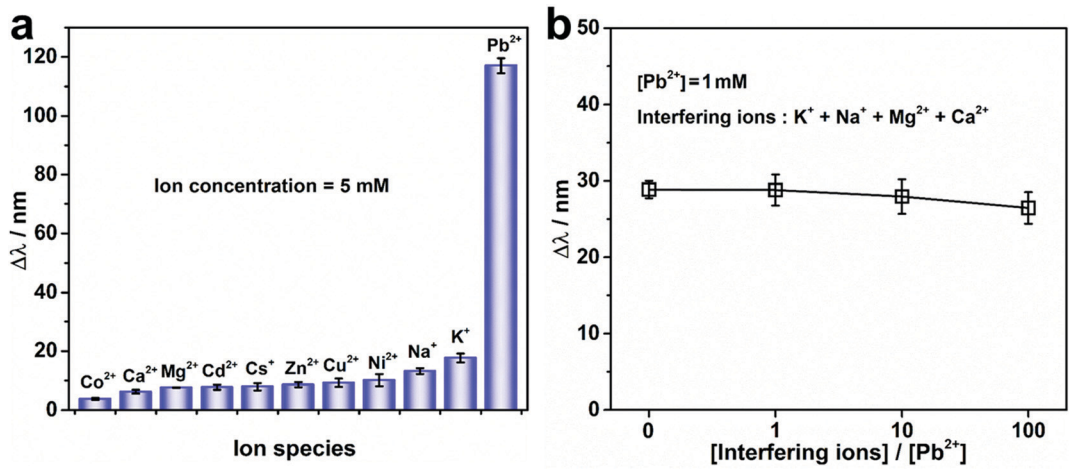

Fig. 5 Selectivity of the PNBC hydrogel sensor toward Pb^{2+}. (a) Effect of ion species on $\Delta\lambda$ in aqueous solutions containing each ion at a concentration of 5 mM at 25 °C. (b) Effect of interfering ions on $\Delta\lambda$ in a 1 mM Pb^{2+} solution containing various interfering ions (K^+, Na^+, Mg^{2+} and Ca^{2+}) in which the concentration of the interfering ions is changed from 1 to 100 mM.

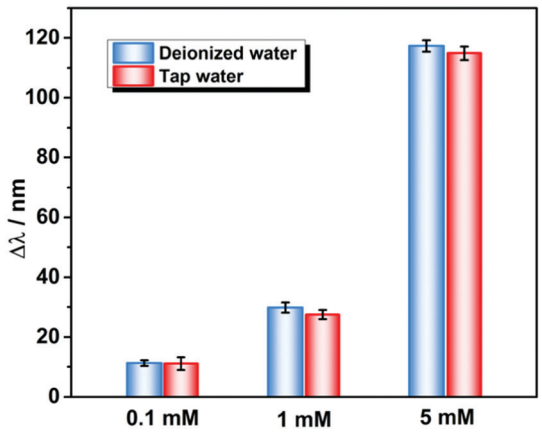

Fig. 6 Detection performance of the PNBC hydrogel sensor toward Pb^{2+} at various concentrations in DI water and tap water.

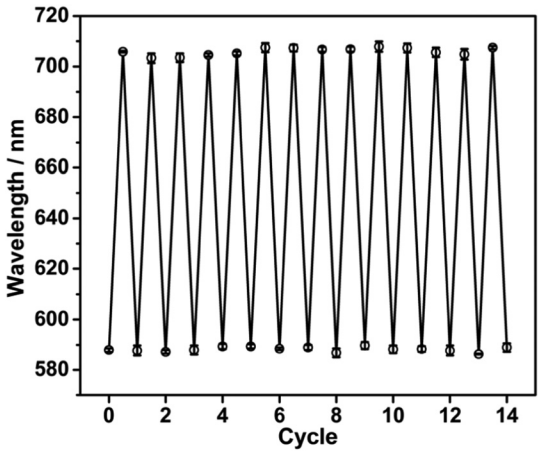

Fig. 7 Reflection wavelengths of the PNBC hydrogel in 5 mM Pb^{2+} solution over 14 consecutive cycles.

$\log K_{Cs^+}$ = 0.88, and $\log K_{Ca^{2+}}$ = 0.5).[61] Therefore, although the ionic radius of K^+, Na^+, and Cs^+ also fit well with the cavity size of 18-crown-6, they are unable to form charged complexes with 18-crown-6 units, and thus cannot trigger structural color changes in the hydrogel. That is to say, the specific recognition and binding of the 18-crown-6 units within the hydrogel toward Pb^{2+} play a crucial role in the highly selective detection and removal of Pb^{2+} in water, which is extremely beneficial for practical applications of the hydrogel in the monitoring of complicated water systems that contain multiple toxic metal ions.

To further validate the effectiveness of the proposed PNBC hydrogel sensor for Pb^{2+} detection in actual environmental water, the PNBC hydrogel was used to detect Pb^{2+} in tap-water samples containing different Pb^{2+} concentrations. As shown in Fig. 6, when the hydrogel was immersed in simulated Pb^{2+}-contaminated tap water containing 0.1, 1, or 5 mM Pb^{2+}, the diffraction wavelength shifts in the simulated tap water are almost the same as those in DI water, indicating that the various cations, anions, and organic compounds in natural water have little effect on the Pb^{2+} detection.[38] Therefore, the PNBC hydrogel developed in this study shows significant promise as an excellent Pb^{2+} sensor in a practical environment.

Reusability of the PNBC photonic hydrogel sensor

As the inclusion constants of B18C6Am/Pb^{2+} complexes are reduced when the surrounding operating temperature is increased, after Pb^{2+} detection or adsorption the used PNBC photonic hydrogel can be completely regenerated by simply increasing the operating temperature and it washing alternately with hot/cold water (25 and 75 °C). To confirm this hypothesis, the diffraction wavelengths of the hydrogel in 14 consecutive Pb^{2+}-detection cycles were measured using a fiber optic spectrometer. As shown in Fig. 7, the as-prepared PNBC hydrogel displays a wide diffraction wavelength change of about 117 nm, and the diffraction wavelengths are 705.0 ± 3.2 nm and 588.0 ± 2.4 nm in the presence and absence of Pb^{2+}, respectively. After repeated use, the diffraction peaks of the hydrogel can be nearly reversed to their original positions (Fig. 7), indicating the high stability and excellent regenerability of the PNBC hydrogel. Compared with conventional regeneration methods of photonic hydrogels that use strong acids and/or other salt solutions,[19,23,56] our presented regeneration strategy shows evident advantages such as its simplicity of operation, its high efficiency and its improved environmental friendliness, which does not bring cause any secondary pollution to the environment.

Pb^{2+} adsorption performance of the PNBC photonic hydrogel sensor

Apart from being a portable colorimetric sensing device for the detection of Pb^{2+}, our developed PNBC hydrogel also shows great promise as an adsorbent for the removal of Pb^{2+} from aqueous solutions. The adsorption performance of the PNBC hydrogel toward Pb^{2+} (C_0 = 0–1650 mg L^{-1}) was also investigated at 25 °C and the results are shown in Fig. 8. The adsorption capacity (q_e, mg g^{-1}) of Pb^{2+} onto the PNBC hydrogel was calculated using the following equation:

$$q_e = (C_0 - C_e) \times V/m \quad (1)$$

where C_0 and C_e (mg L^{-1}) are the initial and equilibrium concentration of Pb^{2+}, respectively, m (g) is the weight of the hydrogel, and V (L) is the volume of Pb^{2+} solution. Upon increasing the Pb^{2+} concentration whilst keeping all the other parameters constant, the q_e increases clearly. At 25 °C (below the VPTT), the copolymer chains of PNBC hydrogel expand and become hydrophilic, and upon increasing the Pb^{2+} concentration more guest Pb^{2+} ions can diffuse into the swollen hydrogel for effective capture and removal through the formation of more B18C6Am/Pb^{2+} host–guest complexes. As observed in Fig. 8a, the 18-crown-6 hosts within the hydrogel are not saturated by Pb^{2+} in water to form complexes. These results indicate that our prepared PNBC hydrogel sensor serves not only as an excellent ion sensor for the specific detection of Pb^{2+} but also as an adsorbent for the timely removal of Pb^{2+} from water.

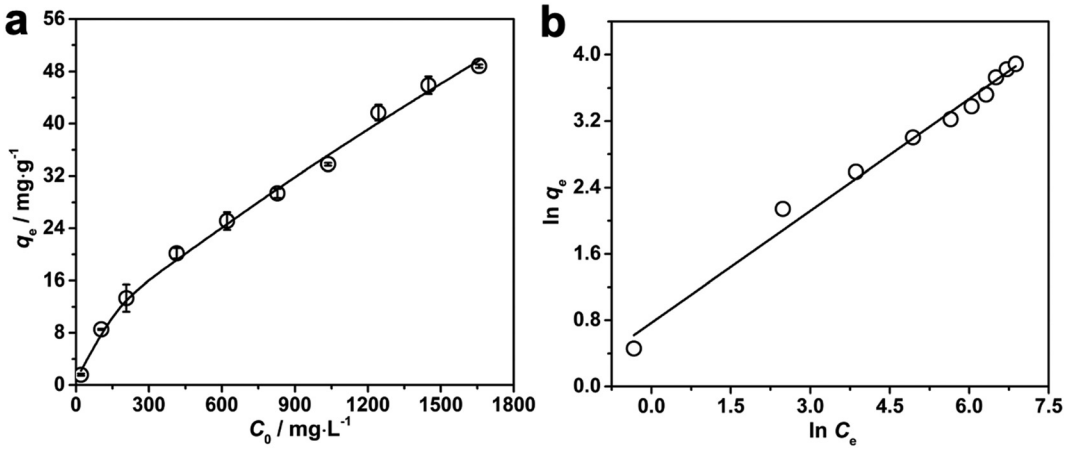

Fig. 8 (a) Adsorption performance of the PNBC photonic hydrogel sensor toward Pb^{2+} in water, where the Pb^{2+} concentration is varied from 0 to 1650 mg L^{-1}; and (b) fitting curve of the Freundlich isotherm model for Pb^{2+} adsorption onto the PNBC photonic hydrogel. The use of the hydrogel is 14 g L^{-1}, the operating temperature is 25 °C, and the pH value is 5.5.

To further elucidate of the adsorption mechanism, two classical adsorption models – the Freundlich and Langmuir isotherm models – were used to study the interactions between Pb^{2+} and the PNBC hydrogel, which are expressed *via* eqn (2) and (3), respectively.

Freundlich model:

$$\ln q_e = \frac{1}{n}\ln C_e + \ln K_F \quad (2)$$

Langmuir model:

$$\frac{C_e}{q_e} = \frac{1}{q_m K_L} + \frac{C_e}{q_m} \quad (3)$$

Here, C_e (mg L^{-1}) is the equilibrium concentration of Pb^{2+} in aqueous solution; q_e and q_m (mg g^{-1}) are the equilibrium and maximum adsorption capacities, respectively; K_F and K_L (L mg^{-1}) are the equilibrium constants for the Freundlich and Langmuir adsorption models, respectively; and n represents a heterogeneity factor related to the adsorption intensity. The isotherm parameters of the two models for Pb^{2+} adsorption by the PNBC hydrogel can be evaluated *via* the slopes and intercepts of the linear plots of C_e/q_e *versus* C_e for the Langmuir model (Fig. S4, ESI†) and $\ln q_e$ *versus* $\ln C_e$ for the Freundlich model (Fig. 8b). The corresponding parameters from these plots are shown in Table 1. The calculated maximum adsorption capacity ($q_{m,cal}$) of the PNBC photonic hydrogel toward Pb^{2+} from the Langmuir model is 60.61 mg g^{-1}, which is larger than the experimental value (48.82 mg g^{-1}). In addition, compared with the correlation coefficient of the Langmuir model (R^2 = 0.8945), the R^2 value of the Freundlich model (R^2 = 0.9850) is higher. That is to say, the Freundlich isotherm model matches better with the adsorption behavior. This implies that Pb^{2+} adsorption onto the PNBC hydrogel occurs mainly on the heterogeneous surface or surface support positions with different affinities. The Freundlich constant n is larger than 1, indicating the high adsorption intensity of the PNBC photonic hydrogel toward Pb^{2+}.[41,44]

Table 1 Isotherm parameters of the Langmuir and Freundlich models for the adsorption of Pb^{2+} onto the PNBC photonic hydrogel

	Langmuir model			Freundlich model		
$q_{m,exp}$ (mg g^{-1})	$q_{m,cal}$ (mg g^{-1})	K_L (L mg^{-1})	R^2	K_F	n	R^2
48.82	60.61	0.00314	0.8945	2.1554	2.222	0.9850

We also summarized the Pb^{2+} detection or adsorption performance achieved by some other materials reported recently, and compared their sensitivity, selectivity, and adsorption performance (Table 2).[6,7,9,10,12,18,35,44,46,60,62] Although few materials or devices show higher detection or adsorption capacities toward Pb^{2+} than our developed PNBC hydrogel, they cannot simultaneously colorimetrically detect and remove Pb^{2+} in water. This hampers their wide applications to some extent. By contrast, our presented PNBC hydrogel is quite portable due to its small size, it enables and sensitive and colorimetric detection by the naked eye, and shows high selectivity toward Pb^{2+} among the coexisting metal ions. Besides, complete regeneration of the functional hydrogel can be achieved by simply changing the operating temperature, which makes it easy to operate and more environmentally friendly.

Conclusions

In summary, a novel ion-responsive photonic hydrogel sensor based on the poly(*N*-isopropylacrylamide-*co*-benzo-18-crown-6 acrylamide) (PNBC) hydrogel with embedded Fe_3O_4 colloidal nanocrystal cluster (CNC) chains has been successfully fabricated through rapid UV curing of a precursor solution in the presence of the self-assembled Fe_3O_4 CNC nanochains, and was used for the highly selective, point-of-care colorimetric detection of Pb^{2+} with the naked eye as well as the removal of Pb^{2+} in water. The pendent 18-crown-6 units in the hydrogel backbone act as ion-responsive receptors for specifically recognizing and binding Pb^{2+} in aqueous solution to form B18C6Am/Pb^{2+} inclusion complexes; concurrently, the poly(*N*-isopropylacrylamide) (PNIPAM) moieties serve as thermosensitive actuators for regulating

Table 2 Comparison of the PNBC photonic hydrogel with previously reported materials in terms of sensitivity, selectivity and absorption performance toward Pb^{2+}

Material	Detection range for Pb^{2+} (mM)	Other detection targets except for Pb^{2+}	q_m (mg g^{-1})	Ref.
MoS_2 quantum dots	From 5×10^{-2} to ~8	Hg^{2+}, Fe^{3+}	—	6
DNAzyme fluorescence biosensor	From 3×10^{-6} to ~5×10^{-3}	—	—	7
PNB hydrogel grating	From 10^{-6} to 10^{-3}	—	—	9
Forward osmosis-driven device	From 10^{-7} to ~1	—	—	10
Functionalized poplar catkin aerogels	—	Cu^{2+}	112.3	12
Pb^{2+} optrode sensor	From 10^{-3} to ~10	—	—	18
PCCA sensor	From 2×10^{-3} to ~10	—	—	35
Magnetic PNB core–shell microspheres	—	—	142.86	44
Microgel-decorated magnetic graphene oxides	—	—	11.76	46
Functionalized lignin	—	Cu^{2+}, Cd^{2+}	91.4	60
Magnetic carbon aerogel	—	*p*-Nitrophenol	68.0	62
PNBC hydrogel	From 10^{-3} to ~10	—	60.61	This study

the inclusion constants of the B18C6Am/Pb^{2+} complexes, thus generating the volume changes and structural colors of the PNBC hydrogel. The fixed orderly Fe_3O_4 CNC chains function as optical signal transmitters that can diffract visible light, thus endowing the hydrogel with brilliant structural colors. The contact time, operating temperature, and solution pH are important factors that affect the Pb^{2+} detection performance of the hydrogel. The developed photonic hydrogel sensor shows highly selective Pb^{2+} detection even in the presence of various interfering ions. In addition, the timely elimination of Pb^{2+} from water is also achieved at room temperature and the adsorption behavior of the hydrogel matches well with the Freundlich isotherm model. Most importantly, our PNBC hydrogel sensor can be completely regenerated by simply changing the operating temperature without compromising its performance. Our developed ion-responsive photonic hydrogel sensor shows great promise in highly selective, portable, visual monitoring and removal of highly toxic Pb^{2+} from contaminated wastewater, which is important for human health and environmental protection.

Author contributions

Zhuo Peng: conceptualization, validation, investigation, data curation, formal analysis, writing – original draft; Hai-Rong Yu: methodology, investigation, funding acquisition, writing – review and editing; Jing-Ya Wen: software, validation; Yan-Lin Wang: data curation; Ting Liang: methodology, supervision; Chang-Jing Cheng: conceptualization, funding acquisition, writing – review and editing.

Conflicts of interest

There are no conflicts to declare.

Acknowledgements

This work was supported by the National Natural Science Foundation of China (21676219), and the Fundamental Research Funds for the Central Universities, Southwest Minzu University (2020NYBPY12).

Notes and references

1 A. T. Jan, M. Azam, K. Siddiqui, A. Ali, I. Choi and Q. M.-R. Haq, *Int. J. Mol. Sci.*, 2015, **16**, 29592–29630.
2 J. Briffa, E. Sinagra and R. Blundell, *Heliyon*, 2020, **6**, e04691–e04717.
3 I. Narin, M. Soylak, L. Elci and M. Dogan, *Talanta*, 2000, **52**, 1041–1046.
4 I. Cesarino, É. T.-G. Cavalheiro and C. M.-A. Brett, *Electroanalysis*, 2010, **22**, 61–68.
5 F. A. Aydin and M. Soylak, *J. Hazard. Mater.*, 2010, **173**, 669–674.
6 P. Sharma and M. S. Mehata, *Mater. Res. Bull.*, 2020, **131**, 110978.
7 T. Fu, S. Ren, L. Gong, H. Meng, L. Cui, R.-M. Kong, X.-B. Zhang and W. Tan, *Talanta*, 2016, **147**, 302–306.
8 A.-L. Chen, H.-R. Yu, X.-J. Ju, R. Xie, W. Wang and L.-Y. Chu, *RSC Adv.*, 2014, **4**, 26030–26037.
9 H.-Y. Peng, W. Wang, F. Gao, S. Lin, L.-Y. Liu, X.-Q. Pu, Z. Liu, X.-J. Ju, R. Xie and L.-Y. Chu, *J. Mater. Chem. C*, 2018, **6**, 11356–11367.
10 Y.-Q. Liu, X.-J. Ju, X.-Q. Pu, S. Wen, W.-Y. Liu, Z. Liu, W. Wang, R. Xie and L.-Y. Chu, *J. Hazard. Mater.*, 2021, **404**, 124157.
11 X.-J. Ju, S.-B. Zhang, M.-Y. Zhou, R. Xie, L. Yang and L.-Y. Chu, *J. Hazard. Mater.*, 2009, **167**, 114–118.
12 H. Li, Z. Wang, X. Liu, F. Cui, C. Chen, Z. Zhang, J. Li, L. Song and R. Bai, *Chem. Phys. Lett.*, 2020, **755**, 137805.
13 M.-Q. Jiang, Q.-P. Wang, X.-Y. Jin and Z.-L. Chen, *J. Hazard. Mater.*, 2009, **170**, 332–339.
14 Z. Li and Y. Yin, *Adv. Mater.*, 2019, **31**, 1807061.
15 G. Isapour and M. Lattuada, *Adv. Mater.*, 2018, **30**, 1707069.
16 J. Hou, M. Li and Y. Song, *Nano Today*, 2018, **22**, 132–144.
17 C. Fenzl, T. Hirsch and O. S. Wolfbeis, *Angew. Chem., Int. Ed.*, 2014, **53**, 3318–3335.
18 C. E. Reese and S. A. Asher, *Anal. Chem.*, 2003, **75**, 3915–3918.
19 J. Qin, B. Dong, L. Cao and W. Wang, *J. Mater. Chem. C*, 2018, **6**, 4234–4242.
20 R. Liu, Z. Cai, Q. Zhang, H. Yuan, G. Zhang and D. Yang, *Sens. Actuators, B*, 2022, **354**, 13126–13135.
21 Z. Cai, Z. A. Sasmal, X. Liu and S. A. Asher, *ACS Sens.*, 2017, **2**, 1474–1481.
22 W. Hong, W. Li, X. Hu, B. Zhao, F. Zhang and D. Zhang, *J. Mater. Chem.*, 2011, **21**, 17193–17201.

23 F. Xiao, Y. Sun, W. Du, W. Shi, Y. Wu, S. Liao, Z. Wu and R. Yu, *Adv. Funct. Mater.*, 2017, **27**, 1702147.
24 J. Ge, Y. Hu and Y. Yin, *Angew. Chem., Int. Ed.*, 2007, **119**, 7572–7575.
25 H. Kim, J. Ge, J. Kim, S. Choi, H. Lee, H. Lee, W. Park, Y. Yin and S. Kwon, *Nat. Photonics*, 2009, **3**, 534–540.
26 Z. Cai, Z. Li, S. Ravaine, M. He, Y. Song, Y. Yin, H. Zheng, J. Teng and A. Zhang, *Chem. Soc. Rev.*, 2021, **50**, 5898–5951.
27 Z.-H. Jia, R. Xie, Y. Qiu, X.-B. Lv, X.-J. Ju, W. Wang, Z. Liu and L.-Y. Chu, *Macromol. Rapid Commun.*, 2021, **42**, 2100200.
28 E. Tian, J. Wang, Y. Zheng, Y. Song, L. Jiang and D. Zhu, *J. Mater. Chem.*, 2008, **18**, 1116–1122.
29 X. Jia, J. Wang, K. Wang and J. Zhu, *Langmuir*, 2015, **31**, 8732–8737.
30 D. Men, H. Zhang, L. Hang, D. Liu, X. Li, W. Cai, Q. Xiong and Y. Li, *J. Mater. Chem. C*, 2015, **3**, 3659–3665.
31 W. Liu, L. Li, S. Liu, B. Liu, Z. Wu and J. Deng, *J. Mater. Chem. C*, 2019, **7**, 8946–8953.
32 C. Wang, F. Xiao, Q. Chen, S. Wang, J. Zhou and Z. Wu, *Analyst*, 2021, **146**, 502–508.
33 Y. Zhang, Y. Sun, J. Liu, P. Guo, Z. Cai and J. Wang, *Sens. Actuators, B*, 2019, **291**, 67–73.
34 Z. Cai, D. H. Kwak, D. Punihaole, Z. Hong, S. S. Velankar, X. Liu and S. A. Asher, *Angew. Chem., Int. Ed.*, 2015, **54**, 13036–13040.
35 J. H. Holtz and S. A. Asher, *Nature*, 1997, **389**, 829–832.
36 J. T. Baca, D. N. Finegold and S. A. Asher, *Analyst*, 2008, **133**, 385–390.
37 M. M. Muscatello and S. A. Asher, *Adv. Funct. Mater.*, 2008, **18**, 1186–1193.
38 D. Kou, W. Ma and S. Zhang, *Adv. Funct. Mater.*, 2020, **31**, 2007032.
39 F.-Y. Lin and L.-P. Yu, *Anal. Methods*, 2012, **4**, 2838–2845.
40 A. V. Goponenko and S. A. Asher, *J. Am. Chem. Soc.*, 2005, **127**, 10753–10759.
41 C. D. Geary, I. Zudans, A. V. Goponenko, S. A. Asher and S. G. Weber, *Anal. Chem.*, 2005, **77**, 185–192.
42 M. Irie, Y. Misumi and T. Tanaka, *Polymer*, 1992, **34**, 4531–4535.
43 T. Ito, Y. Sato, T. Yamaguchi and S.-I. Nakao, *Macromolecules*, 2004, **37**, 3407–3414.
44 Y.-M. Liu, X.-J. Ju, Y. Xin, W.-C. Zheng, W. Wang, J. Wei, R. Xie, Z. Liu and L.-Y. Chu, *ACS Appl. Mater. Interfaces*, 2014, **6**, 9530–9542.
45 Q. Luo, Y. Guan, Y. Zhang and M. Siddiq, *J. Polym. Sci., Part A: Polym. Chem.*, 2010, **48**, 4120–4127.
46 L. Pan, G. Zhai, X. Yang, H. Yu and C. Cheng, *ACS Omega*, 2019, **4**, 3933–3945.
47 K. Yagi, J. A. Ruiz and M. C. Sanchez, *Makromol. Chem., Rapid Commun.*, 1980, **1**, 263–268.
48 R. Ungaro, B. E. Haj and J. Smid, *J. Am. Chem. Soc.*, 1976, **98**, 5198–5202.
49 L. Pan, Z. Peng, H. Yu, T. Liang and C. Cheng, *New J. Chem.*, 2021, **45**, 16511–16519.
50 Y.-Y. Wei, Z. Liu, X.-J. Ju, K. Shi, R. Xie, W. Wang, Z. Cheng and L.-Y. Chu, *Macromol. Chem. Phys.*, 2017, **218**, 1600386.
51 W. Wang, X. Fan, F. Li, J. Qiu, M. M. Umair, W. Ren, B. Ju, S. Zhang and B. Tang, *Adv. Opt. Mater.*, 2018, **6**, 1701093.
52 F. Yan and S. Asher, *Anal. Bioanal. Chem.*, 2007, **387**, 2121–2130.
53 Z. Cai, N. L. Smith, J. T. Zhang and S. A. Asher, *Anal. Chem.*, 2015, **87**, 5013–5025.
54 P. Shen, Y. Zhang, Z. Cai, R. Liu, X. Xu, R. Li, J.-J. Wang and D. A. Yang, *J. Mater. Chem. C*, 2021, **9**, 5840–5857.
55 Z. Cai, L. A. Luck, D. Punihaole, J. Madura and S. A. Asher, *Chem. Sci.*, 2016, **7**, 4557–4562.
56 S. Liu, L. Qin, Z. Ni and M. Chen, *Anal. Methods*, 2017, **9**, 5791–5796.
57 R. D. Shannon and C. T. Prewitt, *Acta Crystallogr.*, 1969, **25**, 925–946.
58 B. Zhang, X. J. Ju, R. Xie, Z. Liu, S. W. Pi and L. Y. Chu, *J. Phys. Chem. B*, 2012, **116**, 5527–5536.
59 S. Ge, J. Li, J. Geng, S. Liu, H. Xu and Z. Gu, *Mater. Horiz.*, 2021, **8**, 1189–1198.
60 C. Jin, G. Liu, G. Wu, S. Huo, Z. Liu and Z. Kong, *Ind. Crops Prod.*, 2020, **155**, 112829.
61 Y. Takeda, R. Kohno, Y. Kudo and N. Fukada, *Bull. Chem. Soc. Jpn.*, 1989, **62**, 999–1003.
62 J. Liu, M. Chen, J. Sheng, J. Xu, Y. Shi and H. Jiang, *Environ. Sci. Water Res. Technol.*, 2022, **8**, 820–835.